In vitro and *in vivo* selective antitumor activity of edelfosine against mantle cell lymphoma and chronic lymphocytic leukemia involving lipid rafts

Faustino Mollinedo[1], Janis de la Iglesia-Vicente[1], Consuelo Gajate[1,2], Ander Estella-Hermoso de Mendoza[3], Janny A. Villa-Pulgarin[1], Mercè de Frias[4], Gaël Roué[5], Joan Gil[4], Dolors Colomer[5], Miguel A. Campanero[6], and Maria J. Blanco-Prieto[3]

[1]Instituto de Biología Molecular y Celular del Cáncer, Centro de Investigación del Cáncer, CSIC-Universidad de Salamanca, Campus Miguel de Unamuno, E-37007 Salamanca, Spain; [2]Unidad de Investigación, Hospital Universitario de Salamanca, Campus Miguel de Unamuno, E-37007 Salamanca, Spain; [3]Departamento de Farmacia y Tecnología Farmacéutica, Facultad de Farmacia, Universidad de Navarra, E-31008 Pamplona, Spain; [4]Departament de Ciències Fisiològiques II, Institut d'Investigació Biomèdica de Bellvitge (IDIBELL)–Universitat de Barcelona, E-08907 L'Hospitalet de Llobregat, Spain ; [5]Unitat d'Hematopatologia, Hospital Clínic, Institut d'Investigacions Biomèdiques August Pi i Sunyer (IDIBAPS)-Universitat de Barcelona, E-08036 Barcelona, Spain; [6]Servicio de Farmacología Clínica, Clínica Universitaria, E-31080 Pamplona, Spain;.

Requests for reprints: Faustino Mollinedo, Instituto de Biología Molecular y Celular del Cáncer, Centro de Investigación del Cáncer, CSIC-Universidad de Salamanca, Campus Miguel de Unamuno, E-37007 Salamanca, Spain. Phone: (+34) 923-294806, Fax: (+34) 923-294795, E-mail: fmollin@usal.es, or Dr. Consuelo Gajate, Unidad de Investigación, Hospital Universitario de Salamanca, Campus Miguel de Unamuno, E-37007 Salamanca, Spain. E-mail: cgajate@usal.es

Grant support: This work was supported by grants from Ministerio de Ciencia e Innovación (SAF2005-04293, SAF2006-8850, SAF2007-61261, SAF2007-60964, PCT-090100-2007-27, SAF2008-02251; and RD06/0020/0014, RD06/0020/0097 and RD06/0020/1037 from Red Temática de Investigación Cooperativa en Cáncer -RTICC-, Instituto de Salud Carlos III -ISCIII-), Fondo de Investigación Sanitaria and European Commission (FIS-FEDER 06/0813), Junta de Castilla y León (CSI01A08, GR15-Experimental Therapeutics and Translational Oncology Program, and Biomedicine Project 2009), Fundación de Investigación Médica Mutua Madrileña (FMM), Fundación "la Caixa" (BM05-30-0), Caja Navarra Foundation, Department of Health of the Government of Navarra ("Ortiz de Landázuri, 2009" project), and AGAUR-Generalitat de Catalunya (2005SGR-00549). C.G. is supported by the Ramón y Cajal Program from the Ministerio de Ciencia e Innovación of Spain. A.E.H.d.M. is supported by a research grant from the Department of Education of the Basque Government (BFI06.37). M.d.F. is a recipient of a fellowship from the AGAUR-Generalitat de Catalunya. G.R. holds a Miguel Servet research contract from ISCIII.

Running title: Antitumor activity of edelfosine against MCL and CLL

Keywords: alkyl-lysophospholipid analog; edelfosine; mantle cell lymphoma; chronic lymphocytic leukemia; apoptosis and lipid rafts.

Translational Relevance

Mantle cell lymphoma (MCL) and chronic lymphocytic leukemia (CLL) lack effective therapy. Synthetic alkyl-lysophospholipid analogs (ALPs) constitute a family of promising anticancer drugs, including miltefosine, perifosine, edelfosine and erucylphosphocholine, that promote apoptosis in a variety of tumor cells. Here, we have found that edelfosine behaves as the most potent ALP in inducing cell death in MCL and CLL cells through co-clustering of Fas/CD95 and rafts. Edelfosine induced a higher apoptotic response than perifosine in MCL and CLL patient-derived cells. Oral administration of edelfosine showed a strong *in vivo* anti-MCL and anti-CLL activity in xenograft mouse models. The drug accumulated in a dramatic and preferential way in the tumor, leading to drastic tumor regression. Our data reported here show a rather selective action of edelfosine against tumor cells, and provide the proof-of-principle and rationale for further clinical evaluation of edelfosine to improve patient outcome in MCL and CLL.

Abstract

Purpose: Mantle cell lymphoma (MCL) and chronic lymphocytic leukemia (CLL) remain B-cell malignancies with limited therapeutic options. The present study investigates the *in vitro* and *in vivo* effect of the phospholipid ether edelfosine (1-*O*-octadecyl-2-*O*-methyl-*rac*-glycero-3-phosphocholine) in MCL and CLL.

Experimental design: A number of cell lines, patient-derived tumor cells and xenografts in severe combined immunodeficiency (SCID) mice were used to examine the anti-MCL and anti-CLL activity of edelfosine. Furthermore, we analyzed edelfosine's mechanism of action and drug biodistribution in MCL and CLL tumor-bearing SCID mice.

Results: Here we have found that the phospholipid ether edelfosine was the most potent alkyl-lysophospholipid analog (ALP) in killing MCL and CLL cells, including patient-derived primary cells, while sparing normal resting lymphocytes. ALPs ranked edelfosine > perifosine >> erucylphosphocholine ≥ miltefosine, in their capacity to elicit apoptosis in MCL and CLL cells. Edelfosine induced co-clustering of Fas/CD95 death receptor and rafts in MCL and CLL cells. Edelfosine was taken up by malignant cells, whereas normal resting lymphocytes hardly incorporated the drug. Raft disruption by cholesterol depletion inhibited drug uptake, Fas/CD95 clustering and edelfosine-induced apoptosis. Edelfosine oral administration showed a potent *in vivo* anticancer activity in MCL and CLL xenograft mouse models, and the drug accumulated dramatically and preferentially in the tumor.

Conclusions: Our data indicate that edelfosine accumulates and kills MCL and CLL cells in a rather selective way, and set co-clustering of Fas/CD95 and lipid rafts as a new framework in MCL and CLL therapy. Our data support a selective antitumor action of edelfosine.

Introduction

Chronic lymphocytic leukemia (CLL), and mantle cell lymphoma (MCL) are two major B-cell-derived neoplasias for which current therapy is not satisfactory, leading in most cases to relapse and eventually to a fatal outcome. This lack of efficient therapy underscores the need for a continued search for novel chemotherapeutic agents. CLL is the most common adult leukemia and is characterized by the progressive accumulation of mature $CD5^+$ B-lymphocytes in the peripheral blood, bone marrow and secondary lymphoid organs. New treatment combinations have incorporated the use of purine analog (fludarabine)-based regimens together with monoclonal antibodies rituximab (anti-CD20) and alemtuzumab (anti-CD52), leading to improved complete response rates and prolonged progression-free survival, but a long-term survival benefit has not been shown (1, 2). MCL is characterized by the chromosomal translocation t(11;14)(q13;q32) resulting in the overexpression of cyclin D1 in mature B-lymphocytes that have a striking tendency to disseminate throughout the body (3). MCL is an aggressive lymphoma with a poor survival outcome and a median survival time of 3.5 years. Conventional chemotherapeutic regimens have been the standard treatment of MCL until the recent incorporation of rituximab, which increases overall survival as well as the response rate and duration. The introduction of stem cell transplantation improves survival, although this therapeutic modality is only applied to younger and fit patients (4). Currently, allogenic bone marrow transplantation represents the only therapy with the potential for a curative approach, although associated with a high rate of complications (4). Therefore, development of novel therapeutic strategies is urgently needed to improve survival in patients with the above B-cell malignancies. In the last years, new strategies have been developed that target crucial cellular pathways, and proteasome inhibition with bortezomib has recently been approved in

relapsed/refractory MCL (5). MCL and CLL cells share a relatively low proliferative index and a poor apoptotic rate (6, 7), and therefore the transforming event is likely a failure in death regulation rather than a loss of growth control. This implies that a therapeutic potential for these diseases may lie in potentiating apoptosis.

Synthetic alkyl-lysophospholipid analogs (ALPs) constitute a family of promising anticancer drugs, including edelfosine, miltefosine, perifosine and erucylphosphocholine, that act at the cell membrane level (8-12). The phospholipid ether edelfosine [1-*O*-octadecyl-2-*O*-methyl-*rac*-glycero-3-phosphocholine, ET-18-OCH_3], considered the ALP prototype, induces selectively apoptosis in tumor cells (13) by recruiting Fas/CD95 death receptor in membrane raft clusters (13-18). Edelfosine was the first antitumor agent shown to act through lipid rafts (15), and these membrane domains have been recently involved in the chemotherapeutic action of some additional antitumor agents (17, 19-23). Lipid rafts are membrane microdomains highly enriched in cholesterol and sphingolipids, and the proteins located in these microdomains are limited in their ability to freely diffuse over the plasma membrane, affecting protein function (24). Recent findings suggest that lipid rafts act as scaffolds where Fas/CD95 and downstream signaling molecules are recruited to trigger apoptosis (16-18, 21, 25).

On these grounds, we hypothesized that MCL and CLL, showing a defective cell death control, could be considered stark examples for the particular proapoptotic features of ALPs. Thus, we addressed the possibility that these B-cell malignancies could be treated by these agents, and examined the putative involvement of lipid rafts in their antitumor action against MCL and CLL.

Materials and methods

Drugs. Edelfosine was from Inkeysa (Barcelona, Spain) and Apointech (Salamanca, Spain). Miltefosine was from Calbiochem (Cambridge, MA). Perifosine and erucylphosphocholine were from Zentaris (Frankfurt, Germany).

Cell lines and primary cells. Detailed information on the cell culture conditions for human MCL (JVM-2, Z-138) and CLL (EHEB) cell lines, and primary cells from CLL and MCL patients is included in Supplementary data.

Apoptosis assay. Quantitation of apoptotic cells was determined by flow cytometry as the percentage of cells in the sub-G_1 region (hypodiploidy) in cell cycle analysis as previously described (26).

To analyze apoptosis in CLL/MCL patient-derived samples, 5 x 10^5 cells were incubated for 48 h with the indicated agents. Cells were then washed in annexin-binding buffer, and incubated in 50 μl annexin-binding buffer with allophycocyanin (APC)–conjugated anti-CD3 and phycoerythrin (PE)–conjugated anti-CD19 antibodies from Becton Dickinson (Mountain View, CA) for 10 min in the dark. Cells were then diluted with annexin-binding buffer to a volume of 150 μl and incubated with 1 μl fluorescein isothiocyanate (FITC)-labeled annexin V (Bender MedSystems, Vienna, Austria) for 15 min in the dark. A total of 10,000 stained cells were then analyzed by flow cytometry on a FACSCalibur flow cytometer, using CellQuest software (Becton Dickinson).

Western blot. Proteins (50 μg) were separated on 12 % SDS-PAGE and transferred onto Immobilon-P membranes (Millipore, Bedford, MA). Membranes were probed with anti-cyclin D1 (DCS-6, Cell Signaling Technologies, Beverly, MA) and

anti-β-actin (Sigma, St. Louis, MO) antibodies. Antibody binding was detected using the ECL detection system (Amersham, Buckinghamshire, UK).

Confocal microscopy. Cells were settled onto poly-L-lysine-coated slides and analyzed with a Zeiss LSM 510 laser scan confocal microscope (Oberkochen, Germany) for membrane raft and Fas/CD95 visualization, using FITC-labeled cholera toxin (FITC-CTx) B subunit (Sigma) and anti-human Fas/CD95 SM1/1 IgG_{2a} mouse monoclonal antibody (Bender Medsystems, Vienna, Austria) followed by CY3-conjugated antimouse antibody (Pharmacia, Uppsala, Sweden), as described (15). Colocalization assays were analyzed by excitation of both fluorochromes in the same section. Negative controls, lacking the primary antibody or using an irrelevant antibody, showed no staining.

Edelfosine uptake. Drug uptake was measured as described previously (13) after incubating 10^6 cells with 10 nmol [^{3}H]edelfosine for 2 h in RPMI-1640/10% FBS, and subsequent exhaustive washing (six times) with PBS + 2% BSA to eliminate the loosely cell surface-bound ether lipid. [^{3}H]edelfosine (specific activity, 42 Ci/mmol) was synthesized by tritiation of the 9-octadecenyl derivative (Amersham Buchler, Braunschweig, Germany).

Cholesterol depletion. 2.5 x 10^5 cells/ml were pretreated with 2.5 mg/ml methyl-β-cyclodextrin (MCD) for 30 min at 37ºC in serum-free medium. Cells were then washed three times and resuspended in complete culture medium before edelfosine addition.

Xenograft mouse model. CB17-severe combined immunodeficiency (SCID) mice (Charles River laboratories, Lyon, France), kept and handled according to institutional guidelines, complying with Spanish legislation under a 12/12 h light/dark cycle at a temperature of 22ºC, received a standard diet and acidified water *ad libitum*. CB17-SCID mice were inoculated subcutaneously into their lower dorsum with 10^7 Z-138 or EHEB cells in 100 μl PBS and 100 μl Matrigel basement membrane matrix (Becton Dickinson). When tumors were palpable, mice were randomly assigned into cohorts of 8-10 mice each, receiving a daily oral administration of edelfosine (30 mg/kg) or an equal volume of vehicle (PBS). The shortest and longest diameter of the tumor were measured with calipers at 2-5-day intervals, and tumor volume (mm^3) was calculated using the following standard formula: (the shortest diameter)^2 × (the longest diameter) × 0.5. Animals were sacrificed, according to institutional guidelines, when the diameter of their tumors reached 3 cm or when significant toxicity was observed. Animal body weight and any sign of morbidity were monitored. Drug treatment lasted for 21 (MCL) and 34 (CLL) days, and mice were killed 24 h after the last drug administration. Then, tumor xenografts were extirpated, measured and weighed, and a necropsy analysis involving tumors and distinct organs was carried out.

Plasma/tissue extraction procedure for edelfosine biodistribution studies. MCL- or CLL-bearing SCID mice were treated with a daily oral administration of edelfosine (30 mg/kg) for 21 (MCL) or 34 (CLL) days. Twenty-four h after the last drug oral administration, blood was collected in EDTA surface-coated tubes and then centrifuged at 2000 *g* for 15 min (4ºC) to collect plasma (100 μl). Then, animals were sacrificed, and distinct organs and tumors were collected and weighed. Tissues and tumors were homogenized in 1-ml PBS (pH 7.4) using a Mini-bead Beater (BioSpect

Products, Inc., Bartelsville, Oklahoma, USA) and centrifuged at 10000 *g* for 10 min. Both plasma and tissue supernatants were collected and stored at -80ºC until high-performance liquid chromatography-mass spectrometry (HPLC-MS) analysis was performed. Ten μg of platelet activating factor (1 mg/ml), used as internal standard, were added onto 100 μl of plasma or tissue/tumor supernatant. 190 μl of a mixture of 1% formic acid/methanol were added in order to precipitate proteins. Samples were vortexed for 1 min and, after centrifugation (20000 *g*, 10 min), 25 μl of the supernatant were analyzed by HPLC-MS.

Quantitative determination of edelfosine by HPLC-MS analysis. The technique used was a slight modification of a previously described method (27), and is described in detail in Supplementary data.

Statistical analysis. All values are expressed as means ± SE. Between-group statistical differences were assessed using the Mann-Whitney test or the Student's *t*-test. A *p* value of less than 0.05 was considered statistically significant.

Results

Edelfosine is the most potent ALP inducing apoptosis in MCL and CLL cells. We have previously found that the ALP edelfosine is effective in inducing apoptosis in a number of leukemic cells through the aggregation of Fas/CD95 in clustered rafts (14-18). Following time-course (Fig. 1A) and dose-response (Fig. 1B) experiments, we found that that ALPs ranked edelfosine > perifosine >> erucylphosphoholine ≥ miltefosine for their capacity to promote apoptosis, assessed as the percentage of cells in the sub-G_1 region (28), in MCL (JVM-2, Z-138) and CLL (EHEB) cell lines. Because

MCL is characterized by cyclin D1 overexpression, we analyzed cyclin D1 levels by Western blot in Z-138 and JVM-2 cells exposed for 1-24 h to 10 μM perifosine or edelfosine. As shown in Fig. 1C, we found only a decrease in cyclin D1 protein level in Z-138 cells after 24-h treatment. However, we detected the cleavage of the typical caspase-3 substrate poly(ADP-ribose) polymerase, as a marker for apoptosis onset, by 6-h treatment in edelfosine- and perifosine-treated Z-138 and JVM-2 cells (data not shown), whereas cyclin D1 protein level remained unaffected (Fig. 1C). It is noteworthy that despite the presence of the t(11;14) in both JVM-2 and Z-138 cell lines, JVM-2 cells harbored a reduced basal cyclin D1 content when compared to Z-138, as assessed by protein and mRNA levels (Fig. 1C, and data not shown). Thus, these results suggest that cyclin D1 modulation is not involved in edelfosine/perifosine antitumor activity in MCL cell lines, and that the decrease in cyclin D1 protein level detected at 24 h (Fig. 1C) was a consequence rather than a cause in edelfosine- and perifosine-induced apoptosis.

Edelfosine was also more active than perifosine against primary malignant cells derived from MCL and CLL patients (Fig. 2). Following a dose-response analysis, we found that edelfosine was significantly more cytotoxic ($p < 0.05$) than perifosine against primary $CD19^+$-CLL cells derived from patients, whereas normal resting $CD3^+$-T lymphocytes from the same patients remained rather resistant (Table 1). This selective action of both edelfosine and perifosine was highlighted when compared to staurosporine that induced apoptosis in both malignant and normal cells at a similar rate (Table 1).

Edelfosine-induced apoptosis in MCL and CLL cells is mediated by lipid rafts. By using the raft marker FITC-CTx B subunit that binds ganglioside G_{M1} (29), mainly

found in rafts (30), we found that 10 μM edelfosine induced co-clustering of lipid rafts and Fas/CD95 in both JVM-2 and EHEB cells (Fig. 3). Furthermore, we found that MCL (JVM-2, Z-138) and CLL (EHEB) cell lines took up high amounts of edelfosine (Fig. 4A), whereas normal resting lymphocytes incorporated negligible amounts of drug (<20 pmol/10^6 cells after 2 h of incubation with 10 nmol [^{3}H]edelfosine). Lipid raft disruption by MCD treatment inhibited drug uptake (Fig. 4A), edelfosine-induced apoptosis (Fig. 4B), as well as Fas/CD95 clustering (data not shown). These data suggest that lipid rafts are essential for edelfosine uptake and edelfosine-induced apoptosis in MCL and CLL cells.

Edelfosine accumulates in MCL and CLL tumors and inhibits human MCL and CLL cell growth in vivo. We next determined whether edelfosine showed *in vivo* anti-human MCL and CLL cell activity. CB17-SCID mice were inoculated with 10^7 Z-138 or EHEB cells for MCL or CLL xenograft animal models. The MCL animal model developed aggressive tumors that were tangible within one week of inoculation, and increased rapidly in a few weeks time (Fig. 5A), whereas CLL tumors grew more slowly (Fig. 5A). Following the development of a palpable tumor, mice were randomized into drug-treated (30 mg/kg edelfosine, daily oral administration) and control (PBS vehicle) groups. Caliper measurements were performed every 2-5 days to calculate tumor volume (Fig. 5A). Oral administration of edelfosine achieved significant MCL and CLL tumor regression (Fig. 5, A-C). When tumor size reached about 10% of body-weight, animals were killed for ethical reasons. This size was approximately reached by day 15 in some of the MCL tumor-bearing mice (Fig. 5A), but this animal model was extended one week more in order to obtain reliable and comparable data with drug-treated animals in which tumor size was decreased by that

time (Fig. 5A). A comparison of tumors isolated from untreated control and drug-treated MCL- and CLL-bearing mice, at the end of treatment, rendered a remarkable anti-MCL and anti-CLL activity of edelfosine, with a reduction of more than 85% in tumor weight and volume in both MCL and CLL animal models (Fig. 5B). Organ examination at necropsy did not reveal any apparent toxicity (data not shown), and there was an evident difference between the highly vascularized tumors from drug-free mice and the pale poorly vascularized tumors from edelfosine-treated mice (Fig. 5C). In addition, MCL tumors were bulky in drug-free mice, but resulted rather flat after edelfosine treatment (Fig. 5C). No significant differences in mean body weight were observed between drug-treated and control animals during the *in vivo* assay (3-5% of body weight loss in the treated groups *vs.* control groups). A drug biodistribution study showed that edelfosine dramatically accumulated in the MCL and CLL tumors (Fig. 5D). Tumor/plasma concentration ratio of edelfosine in the tumor was significantly higher than that detected in both kidney and liver after completion of the experiment in MCL and CLL animal models (Fig. 5D), with a drug mean concentration in plasma of 5.64 μg/ml. In the CLL animal model, we examined the content of edelfosine in a wide variety of distinct organs, and found that the drug was dramatically accumulated in the tumor as compared to lung, heart, spleen, liver, intestine, or kidney (Fig. 5D). Taking together, our data indicate a preferential accumulation of edelfosine in the tumor.

Discussion

The data reported here show that edelfosine behaves as the most potent ALP in killing MCL and CLL cells via a raft-mediated process. Our data indicate that edelfosine is a powerful antitumor agent against MCL and CLL as assessed by *in vitro*,

ex vivo and *in vivo* evidences. In addition, we found a rather selective and dramatic accumulation of edelfosine in MCL and CLL tumor cells in animal models.

Here we found that edelfosine induces the recruitment of Fas/CD95 death receptor in raft aggregates in MCL and CLL cells. Raft disruption by cholesterol depletion in MCL and CLL cells inhibited both edelfosine uptake and drug-induced apoptosis, as well as Fas/CD95 clustering, thus suggesting a major role of rafts in the uptake and antitumor action of edelfosine. Previous reports have shown that MCL and CLL cells express Fas/CD95, but a deficient apoptotic response to the external stimulation of Fas/CD95 by agonistic anti-Fas/CD95 antibodies was reported (7, 31). Unlike the natural ligand FasL/CD95L or agonistic anti-Fas/CD95 antibodies that act through their interaction with the exogenous portion of the Fas/CD95 death receptor, edelfosine induces activation of Fas/CD95 from within the cell independently of its ligand (16, 32). We have previously found that edelfosine is even more efficient than FasL/CD95L in promoting programmed cell death through Fas/CD95 activation by its recruitment in membrane rafts enriched in downstream signaling molecules (14, 16-18, 25, 33). Thus, edelfosine might induce Fas/CD95 activation, even though the receptor is not triggered by its natural ligand or agonistic antibodies.

Using distinct MCL and CLL xenograft mouse models, we found that edelfosine accumulates in high amounts in the tumor tissue and shows a remarkable antitumor activity, leading to dramatic tumor regression. In addition, we consistently found in the MCL and CLL xenograft animal models that tumors became smaller and poorly vascularized. This could be in agreement with reports showing an antiangiogenic effect of edelfosine (34, 35). Thus, further insight into the effect of edelfosine on angiogenesis and how this action affects cancer development is warranted.

Following edelfosine oral administration in non-tumor-bearing SCID mice, we have recently found a rather wide drug distribution pattern to several tissues, including lung, spleen, intestine, liver and kidney (36). In this study, we also found that edelfosine showed a preferential accumulation in the tumor in a MCL-bearing mouse animal model (36). Now, we have largely extended this initial study and analyzed the *in vivo* effect of edelfosine in MCL and CLL animal models. Interestingly, we found here that when SCID mice contained a MCL or CLL tumor, edelfosine distribution was dramatically and significantly shifted towards the tumor (tissue/plasma concentration ratios >16; $p < 0.01$), suggesting a preferential tumor location for edelfosine. Our herein reported *in vivo* data, together with our present and previous *in vitro* determinations in a wide number of malignant and normal cells (14, 16, 17), suggest a rather selective edelfosine uptake and cytotoxic action in tumor cells. The selective action of edelfosine on tumor cells supports its low toxicity. We did not find any apparent damage in the distinct organs analyzed following necropsy analysis in the *in vivo* studies reported here. Lack of toxicity of edelfosine in a rat model has been reported, including no significant cardiotoxicity, hepatotoxicity or renal toxicity (37). Our biodistribution data in the murine models reported here showed a mean concentration of edelfosine in plasma of 5.64 μg/ml (10.77 μM; edelfosine molecular mass, 523.7). Thus, the herein reported *in vitro* effects, rendered by 10 μM edelfosine, were detected at a pharmacologically relevant drug concentration.

Our data constitute the first *in vitro* and *in vivo* evidence for the antitumor action of edelfosine in MCL and CLL, two hematologic malignancies with poor survival outcome. Taken together, the results reported here provide the proof-of-principle and rationale for further clinical evaluation of edelfosine to improve patient outcome in

MCL and CLL. The results reported here also highlight the involvement of lipid rafts in the action of edelfosine on B-cell malignancies, such as MCL and CLL.

Acknowledgments

We are grateful to Alberto Gomez-Alonso, Javier Garcia-Criado and Jose F. Martin-Martin for their help in the *in vivo* assays and for allowing us to use their animal facilities during part of this study.

Disclosure of Potencial Conflicts of Interest

No potential conflicts of interest were disclosed.

References

1. Christian BA, Lin TS. Antibody therapy for chronic lymphocytic leukemia. Semin Hematol 2008;45:95-103.
2. Montserrat E, Moreno C. Chronic lymphocytic leukaemia: a short overview. Ann Oncol 2008;19 Suppl 7:vii320-5.
3. Jares P, Colomer D, Campo E. Genetic and molecular pathogenesis of mantle cell lymphoma: perspectives for new targeted therapeutics. Nat Rev Cancer 2007;7:750-62.
4. Schmidt C, Dreyling M. Therapy of mantle cell lymphoma: current standards and future strategies. Hematol Oncol Clin North Am 2008;22:953-63, ix.
5. Leonard JP, Williams ME, Goy A, Grant S, Pfreundschuh M, Rosen ST, Sweetenham JW. Mantle cell lymphoma: biological insights and treatment advances. Clin Lymphoma Myeloma 2009;9:267-77.

6. Rummel MJ, de Vos S, Hoelzer D, Koeffler HP, Hofmann WK. Altered apoptosis pathways in mantle cell lymphoma. Leuk Lymphoma 2004;45:49-54.

7. Proto-Siqueira R, Panepucci RA, Careta FP, Lee A, Clear A, Morris K, Owen C, Rizzatti EG, Silva WA, Jr., Falcao RP, Zago MA, Gribben JG. SAGE analysis demonstrates increased expression of TOSO contributing to Fas-mediated resistance in CLL. Blood 2008;112:394-7.

8. Gajate C, Mollinedo F. Biological activities, mechanisms of action and biomedical prospect of the antitumor ether phospholipid ET-18-OCH_3 (edelfosine), a proapoptotic agent in tumor cells. Curr Drug Metab 2002;3:491-525.

9. Jendrossek V, Handrick R. Membrane targeted anticancer drugs: potent inducers of apoptosis and putative radiosensitisers. Curr Med Chem Anti-Canc Agents 2003;3:343-53.

10. Mollinedo F, Gajate C, Martin-Santamaria S, Gago F. ET-18-OCH_3 (edelfosine): a selective antitumour lipid targeting apoptosis through intracellular activation of Fas/CD95 death receptor. Curr Med Chem 2004;11:3163-84.

11. Vink SR, van Blitterswijk WJ, Schellens JH, Verheij M. Rationale and clinical application of alkylphospholipid analogues in combination with radiotherapy. Cancer Treat Rev 2007;33:191-202.

12. Mollinedo F. Antitumor ether lipids: proapoptotic agents with multiple therapeutic indications. Expert Opin Ther Patents 2007;17:385-405.

13. Mollinedo F, Fernandez-Luna JL, Gajate C, Martin-Martin B, Benito A, Martinez-Dalmau R, Modolell M. Selective induction of apoptosis in cancer cells by the ether lipid ET-18-OCH_3 (Edelfosine): molecular structure

requirements, cellular uptake, and protection by Bcl-2 and Bcl-X_L. Cancer Res 1997;57:1320-8.

14. Gajate C, Fonteriz RI, Cabaner C, Alvarez-Noves G, Alvarez-Rodriguez Y, Modolell M, Mollinedo F. Intracellular triggering of Fas, independently of FasL, as a new mechanism of antitumor ether lipid-induced apoptosis. Int J Cancer 2000;85:674-82.

15. Gajate C, Mollinedo F. The antitumor ether lipid ET-18-OCH_3 induces apoptosis through translocation and capping of Fas/CD95 into membrane rafts in human leukemic cells. Blood 2001;98:3860-3.

16. Gajate C, Del Canto-Janez E, Acuna AU, Amat-Guerri F, Geijo E, Santos-Beneit AM, Veldman RJ, Mollinedo F. Intracellular triggering of Fas aggregation and recruitment of apoptotic molecules into Fas-enriched rafts in selective tumor cell apoptosis. J Exp Med 2004;200:353-65.

17. Gajate C, Mollinedo F. Edelfosine and perifosine induce selective apoptosis in multiple myeloma by recruitment of death receptors and downstream signaling molecules into lipid rafts. Blood 2007;109:711-9.

18. Gajate C, Gonzalez-Camacho F, Mollinedo F. Involvement of raft aggregates enriched in Fas/CD95 death-inducing signaling complex in the antileukemic action of edelfosine in Jurkat cells. PLoS ONE 2009;4:e5044.

19. Lacour S, Hammann A, Grazide S, Lagadic-Gossmann D, Athias A, Sergent O, Laurent G, Gambert P, Solary E, Dimanche-Boitrel MT. Cisplatin-induced CD95 redistribution into membrane lipid rafts of HT29 human colon cancer cells. Cancer Res 2004;64:3593-8.

20. Delmas D, Rebe C, Micheau O, Athias A, Gambert P, Grazide S, Laurent G, Latruffe N, Solary E. Redistribution of CD95, DR4 and DR5 in rafts accounts

for the synergistic toxicity of resveratrol and death receptor ligands in colon carcinoma cells. Oncogene 2004;23:8979-86.

21. Gajate C, Mollinedo F. Cytoskeleton-mediated death receptor and ligand concentration in lipid rafts forms apoptosis-promoting clusters in cancer chemotherapy. J Biol Chem 2005;280:11641-7.

22. Mollinedo F, Gajate C. Fas/CD95 death receptor and lipid rafts: New targets for apoptosis-directed cancer therapy. Drug Resist Updat 2006;9:51-73.

23. Reis-Sobreiro M, Gajate C, Mollinedo F. Involvement of mitochondria and recruitment of Fas/CD95 signaling in lipid rafts in resveratrol-mediated antimyeloma and antileukemia actions. Oncogene 2009;28:3221-34.

24. Simons K, Toomre D. Lipid rafts and signal transduction. Nat Rev Mol Cell Biol 2000;1:31-9.

25. Gajate C, Gonzalez-Camacho F, Mollinedo F. Lipid raft connection between extrinsic and intrinsic apoptotic pathways. Biochem Biophys Res Commun 2009;380:780-4.

26. Gajate C, Santos-Beneit AM, Macho A, Lazaro M, Hernandez-De Rojas A, Modolell M, Munoz E, Mollinedo F. Involvement of mitochondria and caspase-3 in ET-18-OCH_3-induced apoptosis of human leukemic cells. Int J Cancer 2000;86:208-18.

27. Blanco-Prieto MJ, Campanero MA, Mollinedo F. Quantitative determination of the antitumor alkyl ether phospholipid edelfosine by reversed-phase liquid chromatography-electrospray mass spectrometry: application to cell uptake studies and characterization of drug delivery systems. J Chromatogr B Analyt Technol Biomed Life Sci 2004;810:85-92.

28. Gajate C, Barasoain I, Andreu JM, Mollinedo F. Induction of apoptosis in leukemic cells by the reversible microtubule-disrupting agent 2-methoxy-5-(2',3',4'-trimethoxyphenyl)-2,4,6-cycloheptatrien-1-one: protection by Bcl-2 and Bcl-X_L and cell cycle arrest. Cancer Res 2000;60:2651-9.

29. Schon A, Freire E. Thermodynamics of intersubunit interactions in cholera toxin upon binding to the oligosaccharide portion of its cell surface receptor, ganglioside GM1. Biochemistry 1989;28:5019-24.

30. Harder T, Scheiffele P, Verkade P, Simons K. Lipid domain structure of the plasma membrane revealed by patching of membrane components. J Cell Biol 1998;141:929-42.

31. Plumas J, Jacob MC, Chaperot L, Molens JP, Sotto JJ, Bensa JC. Tumor B cells from non-Hodgkin's lymphoma are resistant to CD95 (Fas/Apo-1)-mediated apoptosis. Blood 1998;91:2875-85.

32. Mollinedo F, Gajate C FasL-independent activation of Fas. *In:* H. Wajant (ed.), Fas Signaling, pp. Chapter 2, pp. 13-27. Georgetown, TX: Landes Bioscience and Springer Science, 2006.

33. Mollinedo F Death receptors in multiple myeloma and therapeutic opportunities. *In:* S. Lonial (ed.), Myeloma Therapy. Pursuing the plasma cell, pp. Chapter 25, pp. 393-419. Totowa, NJ: Humana Press, 2008.

34. Candal FJ, Bosse DC, Vogler WR, Ades EW. Inhibition of induced angiogenesis in a human microvascular endothelial cell line by ET-18-OCH_3. Cancer Chemother Pharmacol 1994;34:175-8.

35. Zerp SF, Vink SR, Ruiter GA, Koolwijk P, Peters E, van der Luit AH, de Jong D, Budde M, Bartelink H, van Blitterswijk WJ, Verheij M. Alkylphospholipids

inhibit capillary-like endothelial tube formation in vitro: antiangiogenic properties of a new class of antitumor agents. Anticancer Drugs 2008;19:65-75.

36. de Mendoza AE, Campanero MA, de la Iglesia-Vicente J, Gajate C, Mollinedo F, Blanco-Prieto MJ. Antitumor alkyl ether lipid edelfosine: tissue distribution and pharmacokinetic behavior in healthy and tumor-bearing immunosuppressed mice. Clin Cancer Res 2009;15:858-64.

37. Mollinedo F, Gajate C, Morales AI, del Canto-Janez E, Justies N, Collia F, Rivas JV, Modolell M, Iglesias A. Novel anti-inflammatory action of edelfosine lacking toxicity with protective effect in experimental colitis. J Pharmacol Exp Ther 2009;329:439-49.

FIGURE LEGENDS

Fig. 1. Induction of apoptosis in MCL and CLL cells by ALPs. MCL (JVM-2, Z-138) and CLL (EHEB) cell lines were incubated for the indicated times with 10 μM of the distinct ALPs edelfosine, perifosine, miltefosine and erucylphosohocholine (erucyl-PC) (A), or for 24 h with different concentrations of the ALPs (B). Apoptosis was then quantitated as percentage of cells in the sub-G_1 region by flow cytometry. Untreated control cells were run in parallel. Data shown are means ± SE of 4 independent determinations. (C) Cells were untreated or treated with 10 μM perifosine or edelfosine for the indicated times, and analyzed by Western blot with anti-cyclin D1 and anti-β-actin antibodies. Immunoblotting of β-actin was used as an internal control for equal protein loading in each lane. Blots are representative of three experiments performed.

Fig. 2. Edelfosine and perifosine kill patient-derived MCL and CLL cells. Primary malignant cells isolated from MCL and CLL patients were incubated for 48 h in the absence (control) or in the presence of 10 μM edelfosine (EDLF) or perifosine (PERF), and then cell viability was assessed as nonapoptotic cells in annexin V analysis by flow cytometry. Data shown are means ± SE of 7 (MCL) or 10 (CLL) independent patients. Asterisks indicate that cell viability in edelfosine- and perifosine-treated cells is significantly different from untreated control cells at $p < 0.05$ (*) and $p < 0.01$ (**) levels by Student's *t*-test.

Fig. 3. Edelfosine-induced co-clustering of Fas/CD95 and rafts in MCL and CLL cells. JVM-2 and EHEB cells were either untreated (Control) or treated with 10 μM edelfosine for 9 h, and then stained with FITC-CTx B subunit to identify lipid rafts

(green fluorescence) and with a specific anti-Fas/CD95 monoclonal antibody, followed by CY3-conjugated anti-mouse Ig antibody (red fluoresecence). Areas of colocalization between membrane rafts and Fas/CD95 in the merge panels are yellow. Images shown are representative of 4 independent experiments. Bar, 10 μm.

Fig. 4. Raft involvement in edelfosine uptake and edelfosine-induced apoptosis. (A) JVM-2, Z-138 and EHEB cells, untreated or pretreated with 2.5 mg/ml MCD for 30 min, were incubated with 10 nmol [^{3}H]edelfosine (0.1 μCi) for 2 h, and then drug uptake was determined. (B) JVM-2, Z-138 and EHEB cells, untreated or pretreated with 2.5 mg/ml MCD for 30 min, were incubated with 10 μM edelfosine for 24 h, and then apoptosis was assessed by flow cytometry as the percentage of hypodiploid (sub-G_1) cells. Data shown are means ± SE of 4 independent determinations. Asterisks indicate values that are significantly different from the corresponding MCD-untreated cells at $p < 0.05$ (*) and $p < 0.01$ (**) levels by Student's *t*-test.

Fig. 5. Edelfosine inhibits human MCL and CLL cell growth *in vivo*. CB17-SCID mice were incoculated s.c. with 10^7 Z-138 or EHEB cells. Daily oral administration of edelfosine (30 mg/kg, $n = 10$ for MCL animal model, and $n = 8$ for CLL animal model) started after the development of a palpable tumor. Tumor size was recorded every 2-5 days. (A) Edelfosine (EDLF) significantly ($p < 0.01$; from day 15 of treatment until the end of the experiment) inhibited MCL and CLL tumor growth compared to the control group treated with vehicle (PBS, $n = 10$ for MCL animal model, and $n = 8$ for CLL animal model). Data shown are means ± SE ($n = 10$, MCL; $n = 8$, CLL). (B) After completion of the *in vivo* assay (22 days for MCL, and 35 days for CLL), control and edelfosine-treated mice were sacrificed and tumors were measured in the distinct mice.

The tumor size and weight values of each single animal (dots) and the average values of each experimental group (horizontal bars) are shown. Asterisks indicate that tumor weight and size values were significantly lower after edelfosine treatment, as compared to control drug-free mice, at $p < 0.01$ (**). (C) Remarkable growth inhibition of MCL and CLL tumors were observed after edelfosine treatment (30 mg/kg). (D) Tissue/plasma concentration ratios, in liver, kidney and tumor, of edelfosine after daily oral administration of edelfosine (30 mg/kg) for 3 weeks in MCL-bearing SCID mice (mean ± SE, $n = 5$), and tissue/plasma concentration ratios, in lung, heart, spleen, liver, intestine, kidney and tumor, of edelfosine after daily oral administration of edelfosine (30 mg/kg) for 34 days in CLL-bearing SCID mice (mean ± SE, $n = 5$). Asterisks indicate that the tumor/plasma ratio values are significantly different from the other tissue/plasma ratios at $p < 0.01$ (**).

Table 1. Selective killing of patient-derived CLL cells by edelfosine, sparing normal cells.

	% Cell viability	
Treatment	$CD19^+$-CLL cells	$CD3^+$-T cells
Edelfosine (10 μM)	60.3 ± 5.6	97.8 ± 1.9
Edelfosine (20 μM)	43.7 ± 4.9	86.5 ± 3.2
Perifosine (10 μM)	73.1 ± 4.8	98.4 ± 1.5
Perifosine (20 μM)	61.0 ± 3.7	90.9 ± 2.8
Staurosporine (0.5 μM)	17.8 ± 6.7	22.5 ± 7.5

Primary lymphocyte cultures from CLL patients were incubated with edelfosine or perifosine for 48 h at the indicated concentrations. Staurosporine was used as a positive control of apoptosis. Percentage of cell viability was measured as nonapoptotic $CD3^+/CD19^-$ T cells or $CD3^-/CD19^+$ B cells from CLL samples in annexin V analysis by flow cytometry. Untreated control $CD19^+$ and $CD3^+$ cells were run in parallel, and showed a cell viability >93% and >98%, respectively. Data are shown as mean values ± SE of 5 independent CLL patients.

Figure 1
Mollinedo et al.

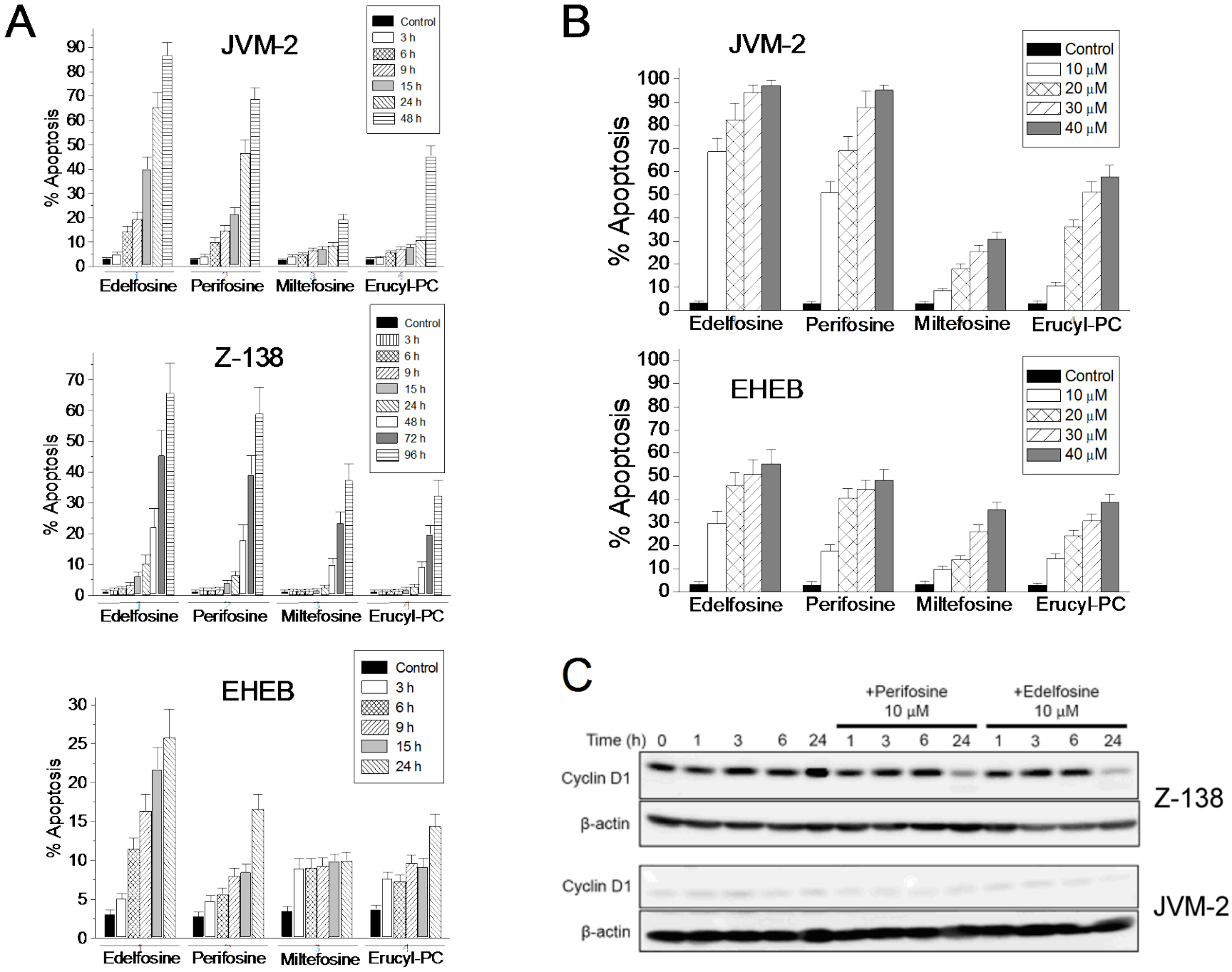

Figure 2
Mollinedo et al.

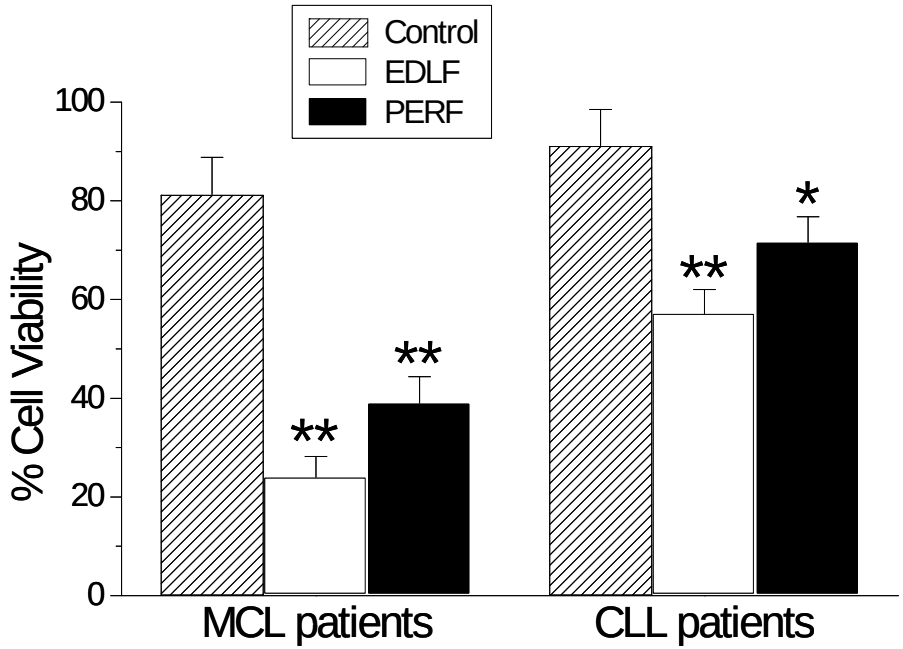

Figure 3
Mollinedo et al.

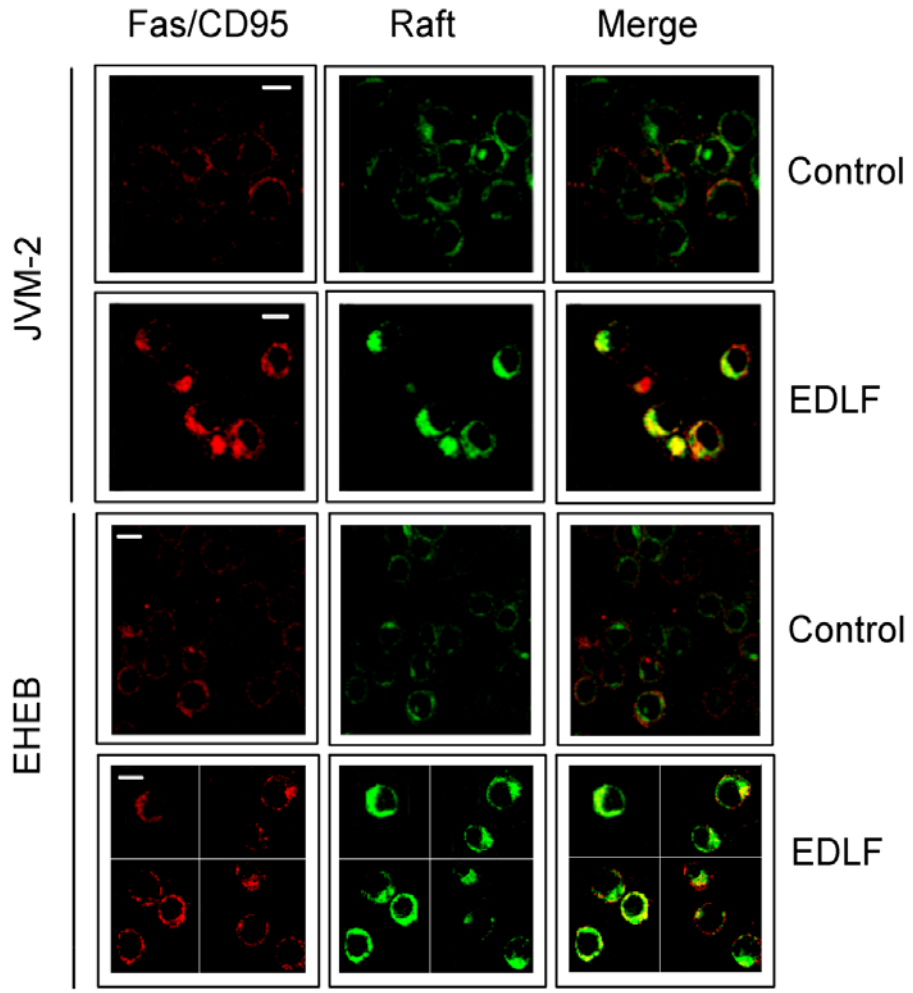

Figure 4
Mollinedo et al.

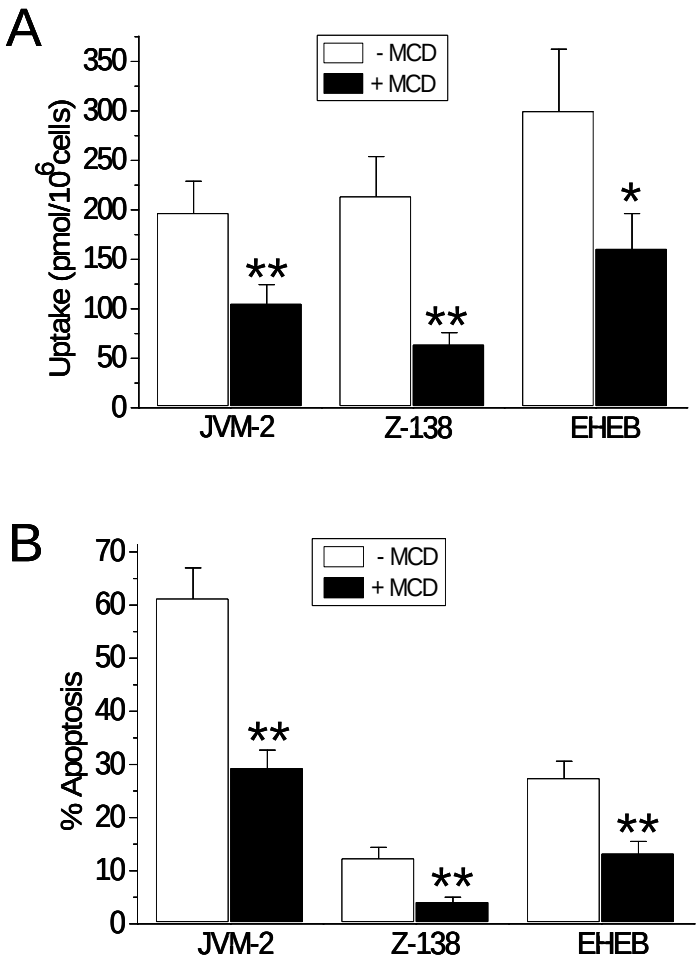

Figure 5
Mollinedo et al.